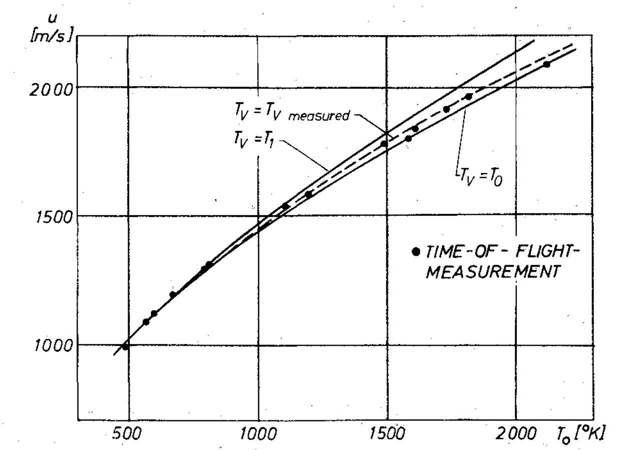

Fig. 3 Flow velocity vs stagnation temperature: comparison—time-of-flight measurement and calculation.

quency times path length. The relative experimental error was estimated to be less than 1%.

Figure 2 shows a typical oscilloscope trace. The upper curve represents two starting pulses having a half-maximum width of 2 μsec. The lower curve shows on the right side the ion signal corresponding to the first upper starting pulse. The measured repetition frequency was equivalent to a time-of-flight of 236.7 μsec. From this, a flow velocity of 1586 m/sec was deduced. A comparison of the experimental flow velocity with data predicted from measurements of stagnation temperature and pitot pressure, has to take into account the vibrational state of the gas. Therefore the vibrational temperature was measured in the same run by the standard electron beam technique.[2,3]

Results and Discussion

Figure 3 shows the results of the time-of-flight velocity measurements. The circles mark the flow velocity data plotted vs the measured stagnation temperature.

The solid curves represent the velocity computed from stagnation temperature and pitot pressure for the case of equilibrium (upper curve) or totally frozen (lower curve) vibrational states.

Most of the experimental data neither lie on the upper nor on the lower curve, but on the dashed curve which represents the flow velocity predicted for the measured vibrational temperature.

It should be noted that the measured vibrational temperature was only about 10% smaller than the stagnation temperature. Although vibrational effects influence the flow velocity only by a small amount, the accuracy of the described method is good enough to indicate even the minute changes in velocity. The good agreement of theory and experiments implies, that the assumptions made for the time-of-flight measurement are valid, namely that the ion velocity is equal to the bulk velocity of the surrounding molecules and that the maximum of the ion signal represents the mean time of arrival of the ions.

References

[1] Koppenwallner, G., Bütefisch, K. A., and Kienappel, K., Forschungsbericht 67-69, 1967, Deutsche Luft- und Raumfahrt, München, Germany; also "Experimentelle Untersuchungen über die hypersonische Düsenströmung bei sehr geringer Gasdichte mit Schwingungs-relaxation," AVA FB 67-40, Sept. 1967, Aerodynamische Versuchsanstalt Göttingen, Germany.

[2] Bütefisch, K. A., Forschungsbericht 69-63, 1969, Deutsche Luft–und Raumfahrt, München, Germany; also "Experimentelle Bestimmung von Rotations- und Schwingungs-temperatur und Dichte mit Hilfe der Elektronenstrahltechnik im Strömungsfeld eines hypersonisch angeströmten Kreiszylinders bei Stautemperaturen von 1100–1800 °K," AVA FB 69-28, June 1969, Aerodynamische Versuchsanstalt Göttingen, Germany.

[3] Muntz, E. P., "Measurement of Rotational Temperature, Vibrational Temperature, and Molecular Concentration, in Nonradiating Flows of Low Density Nitrogen," UTIA Rept. 71, 1961, Inst. of Aerophysics, Univ. of Toronto, Canada.

Radiation from a Porous Wall Heated Internally by a Gas

W. W. Short*
General Research Corporation, Santa Barbara, Calif.

Nomenclature

C_p = heat capacity of gas
d = pore diameter
G = mass flow per unit wall area
h = heat-transfer coefficient in pores
k = thermal conductivity of wall
K = thermal conductivity of gas
l = thickness of wall
n = number of pores per unit wall area
P = porosity of wall = $n\pi d^2/4$
Q = radiation from wall
t = wall temperature
T = gas temperature
T_o = gas temperature entering pores
x = distance from gas inlet surface
ϵ = emissivity of solid
σ = Stefan-Boltzmann constant 1.35×10^{-12} cal/cm²–°K⁴–sec

Dimensionless quantities

$\eta = x/l$
$\theta_T = T/T_o$
$\theta_t = t/T_o$
$\phi = \sigma\epsilon l T_o^3/k(1 - P)$
$\gamma = n\pi dhl/C_pG$
$\lambda = n\pi dhl^2/k(1 - P)$
$E = Q/C_pGT_o$

Introduction

THIS Note investigates a radiation source consisting of a porous wall through which hot gases are forced. The gases enter through one surface, heat the wall internally, and emerge from the opposite surface, which is also the radiating surface. This type of device has applications as a high-altitude or space flare. The usual pyrotechnic flares, in which the fuel is exposed to ambient pressure, do not radiate efficiently and often will not burn at very low pressures. Rocket engines are radiation sources that operate in a low-pressure environment; however they are inefficient radiators because most of the heat of combustion is converted to the directed kinetic energy of the products of combustion. Passing the products of combustion through the small channels of a porous wall retains

Table 1 Constants for evaluating radiation source

Graphite wall	Products of combustion
$K = 1.2\ 10^{-2}$ cal/cm-sec°K	$G = 10^{-2}$ g/s-cm² (assumed)
$\epsilon = 1$	$K = 3\ 10^{-4}$ cal/cm-s-°K
$l = 3.5$ cm	$C_p = 0.3$ cal/g-°K
$n = 3.1\ 10^3$ cm^{-2}	$T_o = 2500$ °K
$p = 0.48$	$\gamma = 1.4\ 10^4$
$d = 1.4\ 10^{-2}$ cm	$\lambda = 2.4\ 10^4$
	$\phi = 6.2$

Received March 12, 1971.
* Member of Technical Staff.

most of the energy as thermal energy which can then be radiated. The analysis presented here derives an expression for the efficiency of converting the internal energy of a hot gas to radiant energy in such devices.

Analysis

The internal energy of the gas is transferred from the gas in the pores to the solid material comprising the wall. The energy is then conducted to the radiating surface. The physical model of the porous wall assumed for this analysis is as follows: 1) The pores are right circular cylinders. 2) Heat is transferred by only three mechanisms; a) convection from the gas to the cylindrical surface of the pores, b) conduction parallel to the pores in the solid, and c) radiation from the solid surface at the exit plane. 3) The process is independent of time.

The energy balance in the solid material is

$$\theta_t'' = \lambda(\theta_t - \theta_T) \tag{1}$$

and the energy balance in the gas is

$$\theta_T' = \gamma(\theta_t - \theta_T) \tag{2}$$

The primes denote differentiation with respect to η. Solving Eqs. (1) and (2) simultaneously for θ_t we obtain

$$\theta_t''' + \gamma\theta_t'' - \lambda\theta_t' = 0 \tag{3}$$

The solution to this third order differential equation is

$$\theta_t = C_1 + C_2e^{\alpha\eta} + C_3e^{\beta\eta} \tag{4}$$

where

$$\alpha,\beta = \tfrac{1}{2}[-\gamma \pm (\gamma^2 + 4\lambda)^{1/2}] \tag{5}$$

The three boundary conditions needed to determine the constants C_1, C_2, and C_3 are a) $\theta_t' = 0$ at $\eta = 0$, b) $\theta_T = 1$ at $\eta = 0$, and c) $\theta_t' = -\phi\theta_t^4$ at $\eta = 1$.

The third boundary condition assumes that the radiating surface acts as a gray body, which is reasonable for the materials usually employed.

The first boundary condition and Eq. (4) give

$$C_2 = -C_3\beta/\alpha \tag{6}$$

The second boundary condition and θ_t'' obtained by differentiating Eq. (4) when substituted into Eq. (1) give

$$C_1 = 1 + C_3\beta(1/\alpha - 1/\beta - \alpha/\lambda + \beta/\lambda) \tag{7}$$

By substituting the values of α and β in this equation, it is discovered that the terms within the parentheses have a value of zero. The constant C_1 is, therefore, equal to one.

The temperature of the wall is

$$\theta_t = 1 - C_3[(\beta/\alpha)e^{\alpha\eta} - e^{\beta\eta}] \tag{8}$$

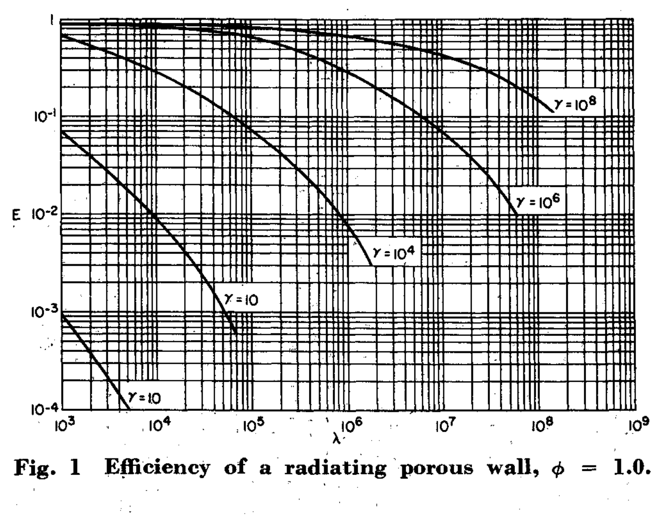

Fig. 1 Efficiency of a radiating porous wall, ϕ = 1.0.

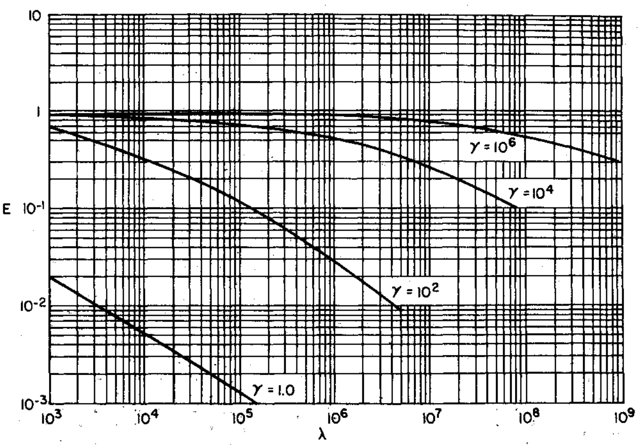

Fig. 2 Efficiency of a radiating porous wall, ϕ = 10³.

The constant, C_3, is not easily eliminated by combining this equation with the third boundary conditions; however it is not the distribution of temperature but the radiant flux from the surface $\eta = 1$ that is the result of interest. Therefore, an equation describing heat transfer will be derived before employing the third boundary condition. The first derivative of θ_t at $\eta = 1$ is proportional to the heat-transfer rate. The radiative transfer can be determined by differentiating Eq. (8) and solving for C_3, then combining the result and Eq. (8) with the third boundary condition. This produces an expression for θ_t', which when expressed in terms of a radiation efficiency is

$$E\lambda/\phi\gamma = [1 + E(\alpha e^{\beta} - \beta e^{\alpha})/\gamma(e^{\beta} - e^{\alpha})]^4 \tag{9}$$

The radiation efficiency is the ratio of the energy radiated from the wall to the latent heat of the gas stream entering the porous wall

$$E = Q/T_0C_pG = -(\gamma\theta_t'/\lambda)_{\eta=1} \tag{10}$$

Curves of the efficiency as a function of λ for several values of γ and ϕ are presented in Figs. 1 and 2.

Example

Porous carbon and graphite are available commercially in a variety of forms for use as filters. One form is a blind end tube, which has been found to be a good radiation source. The physical properties of commercial porous graphite are given in the table following. In the regime of interest, the heat-transfer coefficient is given by the following approximate expression

$$h = 4K/d \tag{11}$$

Using this expression, the constants needed to evaluate a typical radiation source are presented in Table 1. From Figs. 1 and 2 the radiation efficiency can be estimated to be 0.5; therefore Q = 3.8 cal/sec-cm^2.

Discussion

The energy transfer efficiency derived here is only one of several relations needed to design an optimum porous wall radiation source. The other relations are those giving as a function of pressure within the device: the combustion rate of the fuel, the flow rate of combustion products through the wall, and the dimensions of the wall required to prevent failure. Also, if the radiating time is short, the initial transient must be considered. For long duration solid-fueled flares, the internal volume must be sufficient to contain the fuel. The design procedure also depends on the property to be optimized, e.g., total radiation per unit mass of flare or radiation in a spectral interval per unit volume of flare. The design is a trial and error procedure; however, the solution to the energy transfer process presented here makes the mathematics straightforward.